Journal of Robotics and Control (JRC)
Volume 5, Issue 4, 2024
ISSN: 2715-5072, DOI: 10.18196/jrc.v5i4.22256

Parameter Extraction of Triple-diode Photovoltaic Model via RIME Optimizer with Neighborhood Centroid Opposite Solution

Davut Izci [1*], Serdar Ekinci [2], Alfian Ma'arif [3]
[1, 2] Department of Computer Engineering, Batman University, Batman, Turkey
[1] Applied Science Research Center, Applied Science Private University, Amman, 11931, Jordan
[1] MEU Research Unit, Middle East University, Amman 11831, Jordan
[3] Department of Electrical Engineering, Universitas Ahmad Dahlan, Yogyakarta, Indonesia
Email: [1] davutizci@gmail.com, [2] serdar.ekinci@batman.edu.tr, [3] alfianmaarif@ee.uad.ac.id
*Corresponding Author

***Abstract*—In this investigation, a novel application of the RIME optimizer with neighborhood centroid opposite solution is introduced to robustly estimate parameter values for an accurate photovoltaic triple-diode model. The suggested optimizer's performance is rigorously evaluated in comparison to other well-documented methods. The evaluation of the proposed optimizer is conducted using real data from the RTC France solar cell, and the results are assessed through various evaluation metrics, including root mean square error and statistical analyses for multiple independent runs. Specifically, the proposed optimizer demonstrates superior performance by achieving the lowest objective function values compared to other algorithms. Through a comprehensive quantitative and qualitative assessment, it can be inferred that the estimated parameters of the triple-diode model obtained using the proposed optimizer surpass the accuracy of those acquired through other optimization algorithms under consideration.**

***Keywords*—RIME Optimization Algorithm; Triple-diode Model; Parameter Extraction; Neighborhood Centroid Opposition-based Learning.**

I. INTRODUCTION

Solar energy plays a significant role in environmental conservation, social and economic development, job creation, and scientific research, offering numerous advantages as a clean and versatile energy source [1]–[3]. In contrast to dwindling fossil fuel resources, which pose environmental challenges, solar energy stands out as a promising and sustainable alternative [4].

The contemporary applications of solar energy, ranging from solar water heating to solar heating of buildings, solar distillation, solar pumping, solar drying, and solar furnaces, necessitate the development of precise mathematical models for solar systems [5]–[10]. Despite its multifaceted uses, the widespread adoption of solar energy is hindered by the substantial manufacturing and installation costs. Photovoltaic cells, exhibiting nonlinear current-voltage and power-voltage characteristics, further complicate matters by varying their operational efficiency under diverse irradiance and temperature conditions, which fluctuate throughout the day and across seasons [11]. Modeling photovoltaic systems becomes crucial for designing and manufacturing solar technologies, providing essential insights into photovoltaic characteristics under varying conditions and enhancing overall operational efficiency [12]–[18].

In contrast to the ideal solar cell model, which makes use of a pure current source, the practical model has to take into consideration electrical diodes, which stand in for light and current losses. Losses are more pronounced in models that use more diodes. The single diode model incorporates one diode to represent losses in the quasi-neutral zone [19]. The double diode model extends this by incorporating a second diode to represent losses in recombination, especially at lower irradiance [20]. The triple diode model introduces a third diode to account for leakage in grain boundaries within the PV system [21]–[26]. Although increasing the number of diodes improves model accuracy, it simultaneously intensifies model complexity.

Prior research has thoroughly investigated the difficulty of estimating these models' parameters using optimization techniques [27]–[31]. As part of the continued effort, in this study, a commercial silicon R.T.C. France solar cell's triple-diode model characteristics are estimated using a novel optimizer. In terms of the optimizer, an innovative metaheuristic algorithm is introduced, and its impact is assessed on photovoltaic parameter estimation, focusing on the triple-diode model. Specifically, the RIME optimizer [32][33] with neighborhood centroid opposite solution is developed to enhance population dynamics, balance exploration and exploitation, and improve convergence compared to the original RIME.

Results are compared with existing algorithms, including the improved grey wolf optimizer, heap-based optimizer, manta ray foraging optimization, and Harris hawks optimization [5]. Accuracy is evaluated using the root mean square error between real and estimated output currents, while the speed and robustness of the algorithms are compared through convergence curves and statistical analyses, respectively. The current-voltage and power-voltage characteristics of the optimized triple-diode model are discussed across different operating temperatures, revealing the proposed optimizer as a capable and competitive algorithm for triple-diode model parameter extraction in photovoltaic systems.

II. OVERVIEW OF RIME OPTIMIZER

The RIME optimizer, expounded upon by Su et al. in their scholarly work [32], constitutes a fundamental optimization methodology within this study. Drawing inspiration from the evolution process of hoar-frost ice, there are four distinct stages to the RIME optimizer. Commencing with the initialization of a population (X) of search agents in accordance with the hoar-frost ice characteristics, denoted as D representing the problem size [33].

$$X = \begin{bmatrix} x_{11} & x_{12} & \cdots & x_{1D} \\ x_{21} & x_{22} & \cdots & x_{2D} \\ \vdots & \vdots & \ddots & \vdots \\ x_{N1} & x_{N2} & \cdots & x_{ND} \end{bmatrix} \quad (1)$$

These initialized agents serve as the foundation for subsequent operations. Under the condition $r_2 < E$, the method applies the definition in (2) using a soft-rime search strategy that is marked by purposeful randomization to overcome local stagnation:

$$R_{ij}^{new} = R_{best,j} + Rf \times \left(h \times \left(B_{max(i,j)} - B_{min(i,j)}\right) + B_{min(i,j)}\right) \quad (2)$$

where $Rf = r_1 \times cos\theta \times \beta$, $\theta = \pi \cdot (t/(10 \cdot T))$, $\beta = 1 - ((w \cdot t/T)/w)$ and $E = \sqrt{(t/T)}$. Here, $R_{best,j}$ identifies the most effective RIME agent, and R_{ij}^{new} denotes the position of the free particle after motion, with r_1 as a random number between -1 and 1. β symbolizes the ambient conditions of the environment. The variable h denotes a random number, emulating the distance between free particles within a range of 0 to 1. T stands for the maximum iteration count, while t represents the current iteration. E is the chance of collecting free particles, and w is the number of segments in the step function. The goal of the dynamic approach is to avoid settling on less-than-ideal answers too soon by finding a happy medium between exploring and exploiting.

The hard-rime puncture mechanism, inspired by the natural shattering of hoarfrost, causes disturbances among search agents, as mathematically specified in (3):

$$R_{ij}^{new} = R_{best,j}, r_3 < F^{normr}(S_i) \quad (3)$$

Here, $F^{normr}(S_i)$ is the normalized fitness value of the current agent and denotes the probability of the agent experiencing a hard puncture. r_3 is a random number between -1 and 1. The optimization procedure involves positive and selective selection, systematically assessing the fitness values of adapted search agents to update them in the event of improvements. This iterative enhancement contributes to the continual improvement of the overall quality of search agents over time.

III. RIME OPTIMIZER WITH NEIGHBORHOOD CENTROID OPPOSITE SOLUTION

The opposition-based learning (OBL) concept, introduced by Tizhoosh [34], represents a novel paradigm in computational intelligence. OBL involves the computation of inverse points at equidistant positions, selected within the range defined by maximum and minimum boundaries [35]–[45]. This approach has been integrated into various optimization methods [37], [46]–[50]. However, OBL affects only specific individuals within the population and does not leverage the collective search information of the entire population. Addressing this limitation, Rahnamayan proposed the neighborhood centroid opposition-based learning (NCOBL) [51] to utilize comprehensive population search information and extend the group search range, thereby preventing late-stage local optima entrapment.

The NCOBL mechanism employs multiple gravity centers to compute reverse solutions while preserving population diversity. Below is the mathematical model that describes the neighborhood's center of gravity [52]–[55].

$$M_j = \frac{\sum_{j=1}^{D} X_{ij}}{n} \quad (4)$$

Here, M denotes the point of n individual positions in the D-dimensional search space. $\bar{X}_i = 2 \times M - X_i$ stands for the inversion of a point across the whole space where $i = 1,2,\ldots,n$. The motion range of the reverse point within the dynamic boundary is denoted as $x_{ij} \epsilon [a_i, b_j]$, with $a_j = min(x_{ij})$ and $b_j = max\,(x_{ij})$. If the reverse point exceeds the boundary, it is recalculated according to (5).

$$\bar{x}_{ij} = \begin{cases} a_j + rand(0,1) \times (M_j - a_j), if\ \bar{x}_{ij} < a_j \\ M_j + rand(0,1) \times (b_j - M_j), if\ \bar{x}_{ij} > b_j \end{cases} \quad (5)$$

A convergence factor k is introduced, defining the neighborhood barycenter reverse solution as $X_i^* = 2 \times k \times M_i - X_i$ where $i = 1,2,\ldots,n$. The operation of the RIME optimizer with neighborhood centroid opposite solution (NCO-RIME) commences with the execution of the RIME optimizer. The current solution is then updated by evaluating the neighborhood centroid opposite solution. This process iterates until the termination condition is met, and the best solution is obtained. The algorithmic flow is depicted in the presented Fig. 1 flowchart.

IV. MATHEMATICAL REPRESENTATION OF TDM AND ITS FORMULATION AS AN OPTIMIZATION PROBLEM

The triple-diode model (TDM) encapsulates an ideal current source representing the solar cell, three diodes delineating distinct current losses, and series and shunt resistance [5]. The equivalent circuit of the TDM is depicted in Fig. 2.

In this configuration, I_{ph} denotes the photo-generated current, I_{d1} accounts for diffusion current effects, I_{d2} represents recombination current effects, I_{d3} characterizes the impact of grain boundaries and large leakage current, I_{sh} corresponds to the current leakage resistance (shunt resistance, R_{sh}) across the P-N junction of the PV system, and R_s signifies the series resistance associated with current leakage through semiconductor material resistance at neutral regions. The overall output current (I) of the TDM is expressed by (6) and (7).

$$I = I_{ph} - I_{sd1} - I_{sd2} - I_{sd3} - I_{sh} \quad (6)$$

$$I = I_{ph} - I_{sd1}\left(e^{\frac{V+IR_s}{\eta_1 V_t}} - 1\right) - I_{sd2}\left(e^{\frac{V+IR_s}{\eta_2 V_t}} - 1\right) - I_{sd3}\left(e^{\frac{V+IR_s}{\eta_3 V_t}} - 1\right) - \frac{V + IR_s}{R_{sh}} \quad (7)$$

Here, η_1, η_2, and η_3, denote the ideality factors of the diodes D_1, D_2 and D_3, respectively, while V_t represents the thermal voltage (approximately equal to kT/q, where k is Boltzmann's constant, T is the temperature in Kelvin, and q is the elementary charge).

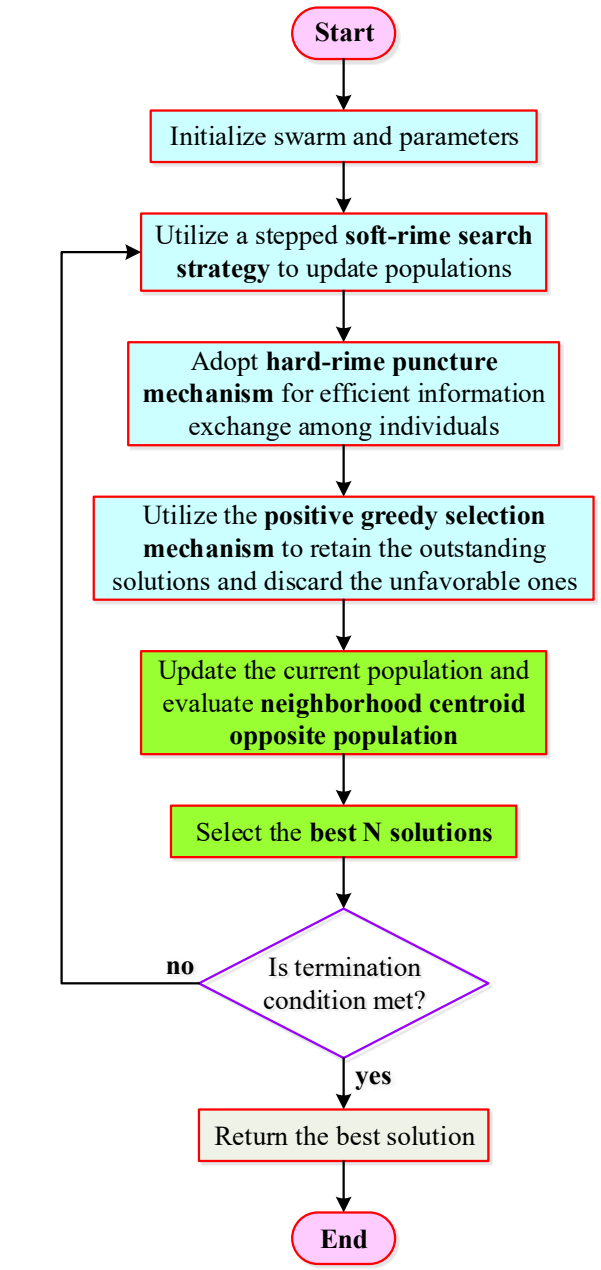

Fig. 1. Flowchart of NCO-RIME algorithm

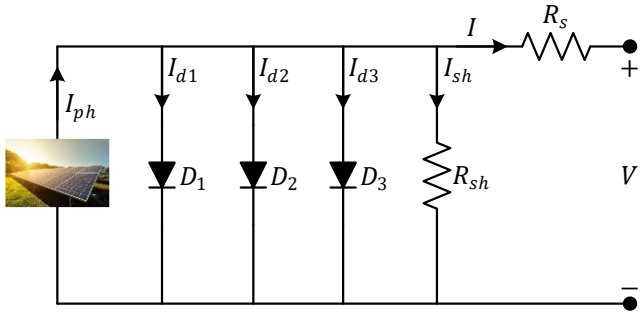

Fig. 2. TDM of PV cell

The TDM involves nine estimated parameters $[R_s, R_{sh}, I_{ph}, I_{sd1}, I_{sd2}, I_{sd3}, \eta_1, \eta_2, \eta_3]$, collectively represented as a vector $x = [x_1, x_2, x_3, x_4, x_5, x_6, x_7, x_8, x_9]$. The objective of this research's optimization challenge is to identify the most favorable values for TDM parameters that minimize the disparity between experimental and predicted output currents. The formulation of the optimization problem's objective function is articulated as follows.

$$f_{TDM}(V, I, X) = I - x_3 - x_4\left(e^{\frac{V+IR_s}{x_7 V_t}} - 1\right) - x_5\left(e^{\frac{V+IR_s}{x_8 V_t}} - 1\right) - x_6\left(e^{\frac{V+IR_s}{x_9 V_t}} - 1\right) - \frac{V + x_1 \mathrm{I}}{x_2} \quad (8)$$

The best estimated parameters are those that minimize the root mean square error (RMSE) for the objective function, expressed as follows [56], [57].

$$RMSE = \sqrt{\frac{1}{N}\sum_{i=1}^{N}(V_m, I_m, \mathrm{X})^2} \quad (9)$$

In here, I_m and V_m stand for the current and voltage that were measured, X for the parameters that were estimated, and N for the maximum amount of data that could be measured.

V. Results and Discussion

A. Parameter Extraction of TDM via NCO-RIME

The RTC France solar cell [58]–[60] serves as the focal point in this investigation. To ensure consistency, a fixed population size of 50 and a maximum iteration limit of 500 were set for all experiments. Additionally, 30 independent runs were conducted to accommodate potential variations in the optimization process. Employing the NCO-RIME, the TDM parameters are meticulously adjusted to optimize its performance. Table I provides the boundaries for the TDM parameters and the corresponding estimated values achieved by NCO-RIME. The results demonstrate the method's capability to accurately estimate the parameters.

TABLE I. Boundaries and Estimated Parameters of TDM

Parameter	Lower Bound	Upper Bound	Estimated by NCO-RIME
I_{ph} (A)	0	1	0.76078
I_{sd1} (μA)	0	1	0.37909
I_{sd2} (μA)	0	1	0.22898
I_{sd3} (μA)	0	1	0.34284
R_s (Ω)	0	0.5	0.036728
R_{sh} (Ω)	0	100	55.36
η_1	1	2	2
η_2	1	2	1.4521
η_3	1	2	2

The convergence performance of NCO-RIME is depicted in Fig. 3. The TDM displays a notable ability to rapidly converge towards the lowest RMSE values, emphasizing the efficiency of NCO-RIME in fine-tuning the TDM parameters. Furthermore, Fig. 4 and Fig. 5 portray the current-voltage (I-V) and power-voltage (P-V) curves of the TDM optimized using NCO-RIME. These figures

compellingly exhibit that the optimized model adeptly captures the solar cell's behavior, as evidenced by the close alignment of the curves with the experimental data.

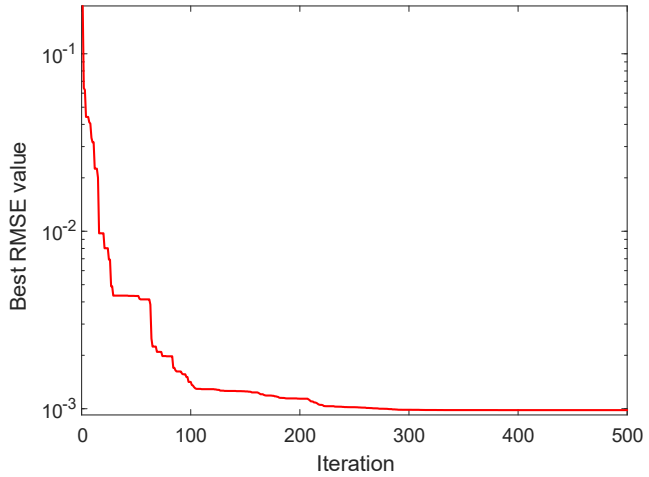

Fig. 3. Convergence behavior of NCO-RIME algorithm

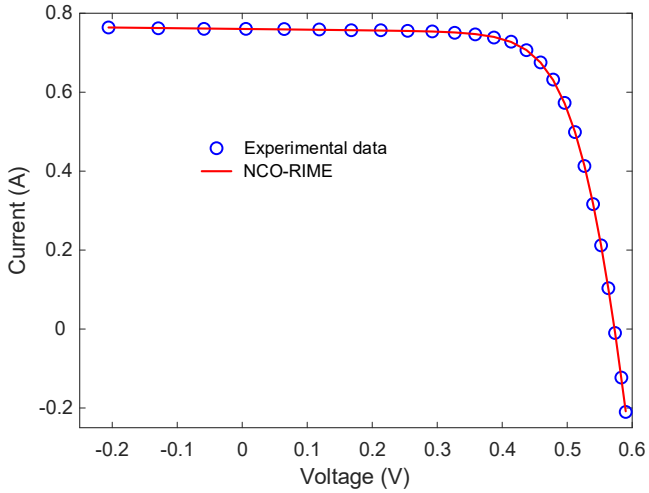

Fig. 4. I-V curves for actual current and TDM current

B. *Comparison with State-of-the-art Metaheuristic Algorithms*

In the comparative evaluation of the NCO-RIME, this study benchmarks its performance against several state-of-the-art metaheuristic algorithms applied to the same PV system. The selected competitive approaches include the improved grey wolf optimizer (I-GWO), heap-based optimizer (HBO), manta ray foraging optimization (MRFO) and Harris hawks optimization (HHO) which are reported in [5].

Table II provides a detailed comparison of the estimated parameters for the TDM across different algorithms. Notably, NCO-RIME demonstrates competitive accuracy in parameter estimation, with RMSE values comparable to or lower than the state-of-the-art approaches.

The comparative statistical analysis in Table III further emphasizes the performance metrics across the algorithms. Metrics including the minimum, maximum, mean, and standard deviation of RMSE are reported. NCO-RIME consistently exhibits minimal RMSE, signifying its robustness and accuracy in parameter estimation. The narrow standard deviation indicates the algorithm's consistency, reinforcing its reliability compared to the competitive approaches. These results collectively highlight the efficacy of NCO-RIME in achieving precise parameter estimation for the TDM, showcasing its potential as a competitive optimization algorithm in the domain of solar PV systems.

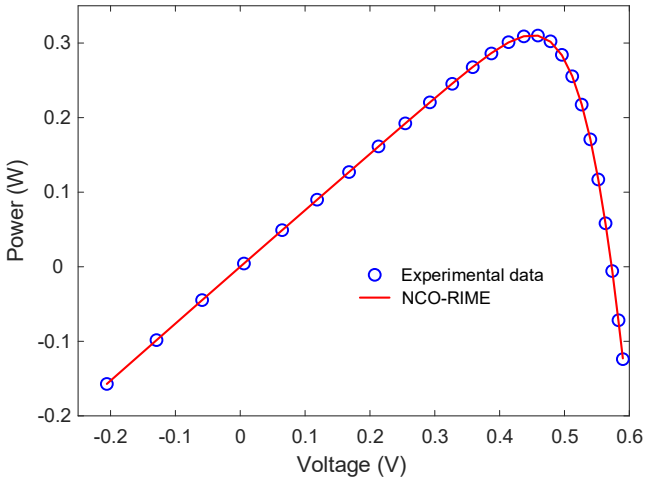

Fig. 5. P-V curves for actual power and TDM power

TABLE II. PARAMETER ESTIMATION OF TDM VIA STATE-OF-THE-ART COMPETITIVE APPROACHES

Parameter	NCO-RIME	I-GWO	HBO	MRFO	HHO
I_{ph} (A)	0.76078	0.7607	0.7608	0.76078	0.764769
I_{sd1} (μA)	0.37909	0.227	0.697	0.0267	3.82
I_{sd2} (μA)	0.22898	0.314	0.0001	0.0154	2.71
I_{sd3} (μA)	0.34284	0.234	1.59472	0.317	1.28
R_s (Ω)	0.036728	0.0367	0.04	0.03634	0.018333
R_{sh} (Ω)	55.36	54.888	59.997	53.9246	92.25011
η_1	2	1.9256	1.009	1.9076	1.882327
η_2	1.4521	1.96	1.0082	1.8674	1.891646
η_3	2	1.45	1.3083	1.475	1.891677
RMSE	**9.8249E−04**	9.8331E−04	1.120E−03	9.86002E−04	7.721E−03

TABLE III. COMPARATIVE STATISTICAL PERFORMANCE EVALUATION OF COMPETITIVE APPROACHES FOR TDM PARAMETER ESTIMATION

Metric	NCO-RIME	I-GWO	HBO	MRFO	HHO
Minimum	**9.8249E−04**	9.83E−04	1.12E−03	9.86E−04	7.7205E−03
Maximum	**9.8426E−04**	9.85E−04	2.4E−03	9.89E−04	1.917E−02
Mean	**9.8343E−04**	9.84E−04	1.606667E−03	9.87E−04	1.17475E−02
Standard Deviation	**6.5370E−07**	6.60404E−07	6.92917E−04	1.25983E−06	6.435824E−03

VI. CONCLUSION

Recognizing the nonlinear characteristics of PV systems and the inherent challenges posed by manufacturers' datasheets, this study explored the application of the RIME optimizer with neighborhood centroid opposite solution for the precise estimation of parameters in a triple-diode PV model. The selection of an appropriate PV model and optimization algorithm is paramount, and the proposed NCO-RIME emerges as a promising solution. Through a comprehensive comparative analysis with established algorithms documented in the literature, the NCO-RIME showcases good performance enhancements, particularly evident in achieving the lowest RMSE values. The evaluation, employing real data from the RTC France solar cell, underscores the efficacy of the proposed optimizer in providing accurate parameter estimates. This superior performance is consistent across various evaluation metrics, affirming its robustness in multiple independent runs. The outcomes of this study substantiate the claim that the NCO-RIME significantly outperforms other algorithms in the realm of PV parameter estimation.

REFERENCES

[1] K. Araújo, J. L. Boucher, and O. Aphale, "A clean energy assessment of early adopters in electric vehicle and solar photovoltaic technology: Geospatial, political and socio-demographic trends in New York," *J. Clean. Prod.*, vol. 216, pp. 99–116, 2019, doi: 10.1016/j.jclepro.2018.12.208.

[2] D. Izci, S. Ekinci, M. Altalhi, M. S. Daoud, H. Migdady, and L. Abualigah, "A new modified version of mountain gazelle optimization for parameter extraction of photovoltaic models," *Electrical Engineering*, 2024, doi: 10.1007/s00202-024-02375-y.

[3] D. Izci, S. Ekinci, and A. G. Hussien, "Efficient parameter extraction of photovoltaic models with a novel enhanced prairie dog optimization algorithm," *Sci. Rep.*, vol. 14, p. 7945, 2024, doi: 10.1038/s41598-024-58503-y.

[4] H. Tyagi, P. R. Chakraborty, S. Powar, and A. K. Agarwal, "Introduction to Solar Energy: Systems, Challenges, and Opportunities," in *Introduction to Solar Energy: Systems, Challenges, and Opportunities*, pp. 3–12, 2020, doi: 10.1007/978-981-15-0675-8_1.

[5] A.-E. Ramadan, S. Kamel, T. Khurshaid, S.-R. Oh, and S.-B. Rhee, "Parameter Extraction of Three Diode Solar Photovoltaic Model Using Improved Grey Wolf Optimizer," *Sustainability*, vol. 13, p. 6963, 2021, doi: 10.3390/su13126963.

[6] A. Al-Subhi, "Efficient mathematical models for parameters estimation of single-diode photovoltaic cells," *Energy Systems*, vol. 15, pp. 275–296, 2024, doi: 10.1007/s12667-022-00542-3.

[7] S. N. Md Sabudin and N. Mohd Jamil, "Mathematical model for predicting the performance of photovoltaic system with delayed solar irradiance," *Kuwait Journal of Science*, vol. 51, p. 100207, 2024, doi: 10.1016/j.kjs.2024.100207.

[8] B. S. Abdullaeva, D. Abduvalieva, F. A. Rakhmatova, and M. E. Yulchiev, "Mathematical model of the solar combined cycle power plant using phase change materials in thermal energy storage system (Thermodynamic analysis)," *International Journal of Thermofluids*, vol. 22, p. 100579, 2024, doi: 10.1016/j.ijft.2024.100579.

[9] O. Bozarov, R. Aliev, A. Kuchkarov, E. Goipov, and M. Kuchkarova, "Results of mathematical modelling of the cooling system for solar panels of a hybrid power plant based on solar and hydraulic energy," *BIO Web Conf.*, vol. 84, p. 05023, 2024, doi: 10.1051/bioconf/20248405023.

[10] J. Wu, W. An, and Y. Zhang, "The regulating effect of nanoparticle concentration on the performance in HPV/D solar system with nanofluids spectral splitting technique," *Appl. Therm. Eng.*, vol. 243, p. 122594, 2024, doi: 10.1016/j.applthermaleng.2024.122594.

[11] A. Sharma, A. Sharma, M. Averbukh, V. Jately, B. Azzopardi, "An Effective Method for Parameter Estimation of a Solar Cell," *Electronics (Basel)*, vol. 10, p. 312, 2021, doi: 10.3390/electronics10030312.

[12] A. Ramadan, S. Kamel, M. H. Hassan, E. M. Ahmed, and H. M. Hasanien, "Accurate Photovoltaic Models Based on an Adaptive Opposition Artificial Hummingbird Algorithm," *Electronics (Basel)*, vol. 11, p. 318, 2022, doi: 10.3390/electronics11030318.

[13] D. Ben Hmamou *et al*., "Experimental characterization of photovoltaic systems using sensors based on MicroLab card: Design, implementation, and modeling," *Renew. Energy,* vol. 223, p. 120049, 2024, doi: 10.1016/j.renene.2024.120049.

[14] B. Taghezouit, F. Harrou, Y. Sun, and W. Merrouche, "Model-based fault detection in photovoltaic systems: A comprehensive review and avenues for enhancement," *Results in Engineering*, vol. 21, p. 101835, 2024, doi: 10.1016/j.rineng.2024.101835.

[15] H. Abdulla, A. Sleptchenko, and A. Nayfeh, "Photovoltaic systems operation and maintenance: A review and future directions," *Renewable and Sustainable Energy Reviews*, vol. 195, p. 114342, 2024, doi: 10.1016/j.rser.2024.114342.

[16] A. Mohammad Rafiei and A. Askarzadeh, "An experimental study for efficiency modeling of grid-connected photovoltaic system," *Energy Sources, Part A: Recovery, Utilization, and Environmental Effects*, vol. 46, pp. 475–492, 2024, doi: 10.1080/15567036.2023.2287090.

[17] T. Al Smadi, A. Handam, K. S. Gaeid, A. Al-Smadi, Y. Al-Husban, and A. smadi Khalid, "Artificial intelligent control of energy management PV system," *Results in Control and Optimization*, vol. 14, p. 100343, 2024, doi: 10.1016/j.rico.2023.100343.

[18] I. Diab, N. Damianakis, G. R. Chandra-Mouli, and P. Bauer, "A shared PV system for transportation and residential loads to reduce curtailment and the need for storage systems," *Appl. Energy,* vol. 353, p. 122131, 2024, doi: 10.1016/j.apenergy.2023.122131.

[19] H. Sharadga, S. Hajimirza, and E. P. T. Cari, "A Fast and Accurate Single-Diode Model for Photovoltaic Design," *IEEE J. Emerg. Sel. Top Power Electron.*, vol. 9, pp. 3030–3043, 2021, doi: 10.1109/JESTPE.2020.3016635.

[20] G. Sulyok and J. Summhammer, "Extraction of a photovoltaic cell's double-diode model parameters from data sheet values," *Energy Sci. Eng.*, vol. 6, pp. 424–436, 2018, doi: 10.1002/ese3.216.

[21] J. Montano, A. F. T. Mejia, A. A. Rosales Muñoz, F. Andrade, O. D. Garzon Rivera, and J. M. Palomeque, "Salp Swarm Optimization Algorithm for Estimating the Parameters of Photovoltaic Panels Based on the Three-Diode Model," *Electronics (Basel)*, vol. 10, p. 3123, 2021, doi: 10.3390/electronics10243123.

[22] P. A. Kumari *et al*., "Application of DSO algorithm for estimating the parameters of triple diode model-based solar PV system," *Sci. Rep.*, vol. 14, p. 3867, 2024, doi: 10.1038/s41598-024-53582-3.

[23] A. Wadood, E. Ahmed, S. Khan, and H. Ali, "Fraction order particle swarm optimization for parameter extraction of triple-diode photovoltaic models," *Engineering Research Express*, vol. 6, p. 025316, 2024, doi: 10.1088/2631-8695/ad3f6f.

[24] R. Kumar and A. Kumar, "Effective-diode-based analysis of industrial solar photovoltaic panel by utilizing novel three-diode solar cell model against conventional single and double solar cell," *Environmental Science and Pollution Research*, vol. 31, pp. 25356–25372, 2024, doi: 10.1007/s11356-024-32474-z.

[25] İ. Çetinbaş, "Parameter Extraction of Single, Double, and Triple-Diode Photovoltaic Models Using the Weighted Leader Search Algorithm," *Global Challenges*, vol. 8, no. 5, p. 2300355, 2024, doi: 10.1002/gch2.202300355.

[26] M. Gafar, R. A. El-Sehiemy, H. M. Hasanien, and A. Abaza, "Optimal parameter estimation of three solar cell models using modified spotted hyena optimization," *J. Ambient Intell. Humaniz Comput.*, vol. 15, no. 1, pp. 361-372, 2024, doi: 10.1007/s12652-022-03896-9.

[27] H. Krishnan, M. S. Islam, M. A. Ahmad, and M. I. M. Rashid, "Parameter identification of solar cells using improved Archimedes Optimization Algorithm," *Optik (Stuttg)*, vol. 295, p. 171465, 2023 doi: 10.1016/j.ijleo.2023.171465.

[28] H. Ben Aribia *et al*., "Growth Optimizer for Parameter Identification of Solar Photovoltaic Cells and Modules," *Sustainability*, vol. 15, p. 7896, 2023, doi: 10.3390/su15107896.

[29] R. Mohamed, M. Abdel-Basset, K. M. Sallam, I. M. Hezam, A. M. Alshamrani, and I. A. Hameed, "Novel hybrid kepler optimization algorithm for parameter estimation of photovoltaic modules," *Sci. Rep.*, vol. 14, p. 3453, 2024, doi: 10.1038/s41598-024-52416-6.

[30] M. Qaraad, S. Amjad, N. K. Hussein, M. A. Farag, S. Mirjalili, and M. A. Elhosseini, "Quadratic interpolation and a new local search approach to improve particle swarm optimization: Solar photovoltaic parameter estimation," *Expert Syst. Appl.*, vol. 236, p. 121417, 2024, doi: 10.1016/j.eswa.2023.121417.

[31] D. İzci, S. Ekinci, and M. Güleydin, "Improved Reptile Search Algorithm for Optimal Design of Solar Photovoltaic Module," *Computer Science IDAP-2023*, pp. 172–179, 2023.

[32] H. Su *et al*., "RIME: A physics-based optimization," *Neurocomputing*, vol. 532, pp. 183–214, 2023, doi: 10.1016/j.neucom.2023.02.010.

[33] S. Ekinci, Ö. Can, M. Ş. Ayas, D. Izci, M. Salman, and M. Rashdan, "Automatic Generation Control of a Hybrid PV-Reheat Thermal Power System Using RIME Algorithm," *IEEE Access*, vol. 12, pp. 26919–26930, 2024, doi: 10.1109/ACCESS.2024.3367011.

[34] H. R. Tizhoosh, "Opposition-Based Learning: A New Scheme for Machine Intelligence," in *International Conference on Computational Intelligence for Modelling, Control and Automation and International Conference on Intelligent Agents, Web Technologies and Internet Commerce (CIMCA-IAWTIC'06)*, pp. 695–701, 2005, doi: 10.1109/CIMCA.2005.1631345.

[35] D. Izci, S. Ekinci, E. Eker, and M. Kayri, "Improved Manta Ray Foraging Optimization Using Opposition-based Learning for Optimization Problems," in *2020 International Congress on Human-Computer Interaction, Optimization and Robotic Applications (HORA)*, pp. 1–6, 2020, doi: 10.1109/HORA49412.2020.9152925.

[36] S. Ekinci, Ö. Can, and D. Izci, "Controller design for automatic voltage regulator system using modified opposition-based weighted mean of vectors algorithm," *International Journal of Modelling and Simulation*, pp. 1–18, 2023, doi: 10.1080/02286203.2023.2274254.

[37] D. Izci, S. Ekinci, E. Eker, and M. Kayri, "Augmented hunger games search algorithm using logarithmic spiral opposition-based learning for function optimization and controller design," *Journal of King Saud University - Engineering Sciences*, 2022, doi: 10.1016/j.jksues.2022.03.001.

[38] D. Izci, S. Ekinci, E. Eker, and L. Abualigah, "Opposition-Based Arithmetic Optimization Algorithm with Varying Acceleration Coefficient for Function Optimization and Control of FES System," in *Proceedings of International Joint Conference on Advances in Computational Intelligence*, pp. 283–293, 2022, doi: 10.1007/978-981-19-0332-8_20.

[39] D. Izci, S. Ekinci, E. Eker, and M. Kayri, "A novel modified opposition-based hunger games search algorithm to design fractional order proportional-integral-derivative controller for magnetic ball suspension system," *Advanced Control for Applications*, vol. 4, p. e96, 2022, doi: 10.1002/adc2.96.

[40] S. Ekinci, D. Izci, L. Abualigah, A. G. Hussien, C.-L. Thanh, and S. Khatir, "Revolutionizing Vehicle Cruise Control: An Elite Opposition-Based Pattern Search Mechanism Augmented INFO Algorithm for Enhanced Controller Design," *International Journal of Computational Intelligence Systems*, vol. 16, p. 129, 2023, doi: 10.1007/s44196-023-00304-8.

[41] D. Izci, S. Ekinci, E. Eker, and A. Demirören, "Biomedical Application of a Random Learning and Elite Opposition-Based Weighted Mean of Vectors Algorithm with Pattern Search Mechanism," *Journal of Control, Automation and Electrical Systems*, vol. 34, pp. 333–343, 2023, doi: 10.1007/s40313-022-00959-2.

[42] H. Özmen, S. Ekinci, and D. Izci, "Boosted arithmetic optimization algorithm with elite opposition-based pattern search mechanism and its promise to design microstrip patch antenna for WLAN and WiMAX," *International Journal of Modelling and Simulation*, pp. 1–16, 2023, doi: 10.1080/02286203.2023.2196736.

[43] S. Ekinci, D. Izci, L. Abualigah, and R. A. Zitar, "A Modified Oppositional Chaotic Local Search Strategy Based Aquila Optimizer to Design an Effective Controller for Vehicle Cruise Control System," *J. Bionic. Eng.*, vol. 20, pp. 1828–1851, 2023, doi: 10.1007/s42235-023-00336-y.

[44] L. Abualigah, S. Ekinci, D. Izci, and R. A. Zitar, "Modified Elite Opposition-Based Artificial Hummingbird Algorithm for Designing FOPID Controlled Cruise Control System," *Intelligent Automation & Soft Computing*, vol. 38, pp. 169–183, 2023, doi: 10.32604/iasc.2023.040291.

[45] D. Izci, S. Ekinci, E. Eker, and A. Dundar, "Improving Arithmetic Optimization Algorithm Through Modified Opposition-based Learning Mechanism," in *2021 5th International Symposium on Multidisciplinary Studies and Innovative Technologies (ISMSIT)*, pp. 1–5, 2021, doi: 10.1109/ISMSIT52890.2021.9604531.

[46] T. J. Choi, J. Togelius, and Y.-G. Cheong, "A Fast and efficient stochastic opposition-based learning for differential evolution in numerical optimization," *Swarm Evol. Comput.*, vol. 60, p. 100768, 2021, doi: 10.1016/j.swevo.2020.100768.

[47] N. Rizvi, D. Ramesh, P. C. S. Rao, and K. Mondal, "Intelligent Salp Swarm Scheduler With Fitness Based Quasi-Reflection Method for Scientific Workflows in Hybrid Cloud-Fog Environment," *IEEE Transactions on Automation Science and Engineering*, vol. 20, pp. 862–877, 2023, doi: 10.1109/TASE.2022.3170549.

[48] M. Elsisi, "Improved grey wolf optimizer based on opposition and quasi learning approaches for optimization: case study autonomous vehicle including vision system," *Artif. Intell. Rev.*, vol. 55, no. 7, pp. 5597-5620, 2022, doi: 10.1007/s10462-022-10137-0.

[49] T. Si *et al*., "PCOBL: A Novel Opposition-Based Learning Strategy to Improve Metaheuristics Exploration and Exploitation for Solving Global Optimization Problems," *IEEE Access*, vol. 11, pp. 46413–46440, 2023, doi: 10.1109/ACCESS.2023.3273298.

[50] S. Ekinci, D. Izci, E. Eker, L. Abualigah, C.-L. Thanh, and S. Khatir, "Hunger games pattern search with elite opposite-based solution for solving complex engineering design problems," *Evolving Systems*, pp. 1-26, 2023, doi: 10.1007/s12530-023-09526-9.

[51] S. Rahnamayan, J. Jesuthasan, F. Bourennani, H. Salehinejad, and G. F. Naterer, "Computing opposition by involving entire population," in *2014 IEEE Congress on Evolutionary Computation (CEC)*, pp. 1800–1807, 2014, doi: 10.1109/CEC.2014.6900329.

[52] B. Li, L.-G. Gong, and Y. Li, "A Novel Artificial Bee Colony Algorithm Based on Internal-Feedback Strategy for Image Template Matching," *The Scientific World Journal*, vol. 2014, pp. 1–14, 2014, doi: 10.1155/2014/906861.

[53] C. Fan, Y. Zhou, and Z. Tang, "Neighborhood centroid opposite-based learning Harris Hawks optimization for training neural networks," *Evol. Intell.,* vol. 14, pp. 1847-1867, 2020.

[54] L. Liao and Y. Zhou, "A Neighborhood Centroid Opposition-Based Grasshopper Optimization Algorithm," *J. Phys. Conf. Ser.,* vol. 1176, p. 032044, 2019, doi: 10.1088/1742-6596/1176/3/032044.

[55] S. Rahnamayan, J. Jesuthasan, F. Bourennani, G. F. Naterer, and H. Salehinejad, "Centroid Opposition-Based Differential Evolution," *International Journal of Applied Metaheuristic Computing*, vol. 5, pp. 1–25, 2014, doi: 10.4018/ijamc.2014100101.

[56] M. Abdel-Basset, R. Mohamed, A. El-Fergany, M. Abouhawwash, and S. S. Askar, "Parameters Identification of PV Triple-Diode Model Using Improved Generalized Normal Distribution Algorithm," *Mathematics*, vol. 9, p. 995, 2021, doi: 10.3390/math9090995.

[57] S. Ekinci, D. Izci, and A. G. Hussien, "Comparative analysis of the hybrid gazelle-Nelder–Mead algorithm for parameter extraction and optimization of solar photovoltaic systems," *IET Renewable Power Generation*, vol. 18, pp. 959–978, 2024, doi: 10.1049/rpg2.12974.

[58] D. Izci, S. Ekinci, S. Dal, and N. Sezgin, "Parameter Estimation of Solar Cells via Weighted Mean of Vectors Algorithm," in *2022 Global Energy Conference (GEC)*, pp. 312–316, 2022, doi: 10.1109/GEC55014.2022.9986943.

[59] H. A. Ismail and A. A. Z. Diab, "An efficient, fast, and robust algorithm for single diode model parameters estimation of photovoltaic solar cells," *IET Renewable Power Generation*, vol. 18, pp. 863–874, 2024, doi: 10.1049/rpg2.12958.

[60] N. J. Mlazi, M. Mayengo, G. Lyakurwa, and B. Kichonge, "Mathematical modeling and extraction of parameters of solar photovoltaic module based on modified Newton–Raphson method," *Results Phys*., vol. 57, p. 107364, 2024, doi: 10.1016/j.rinp.2024.107364.